

Phylogenomics Places Orphan Protistan Lineages in a Novel Eukaryotic Super-Group

Matthew W. Brown^{1,2}, Aaron A. Heiss^{3,4}, Ryoma Kamikawa⁵, Yuji Inagaki^{6,7}, Akinori Yabuki⁸, Alexander K. Tice^{1,2}, Takashi Shiratori⁶, Ken-Ichiro Ishida⁶, Tetsuo Hashimoto^{6,7}, Alastair G.B. Simpson^{3,*}, and Andrew J. Roger^{9,*}

¹Department of Biological Sciences, Mississippi State University, USA

²Institute for Genomics, Biocomputing & Biotechnology, Mississippi State University, USA

³Department of Biology, and Centre for Comparative Genomics and Evolutionary Bioinformatics, Dalhousie University, Halifax, Nova Scotia, Canada

⁴Department of Invertebrate Zoology and Sackler Institute for Comparative Genomics, American Museum of Natural History, New York, New York, USA

⁵Graduate School of Human and Environmental Studies, Graduate School of Global Environmental Studies, Kyoto University, Japan

⁶Graduate School of Life and Environmental Sciences, University of Tsukuba, Ibaraki, Japan

⁷Center for Computational Sciences, University of Tsukuba, Ibaraki, Japan

⁸Japan Agency for Marine-Earth Science and Technology (JAMSTEC), Yokosuka, Kanagawa, Japan

⁹Department of Biochemistry and Molecular Biology, and Centre for Comparative Genomics and Evolutionary Bioinformatics, Dalhousie University, Halifax, Nova Scotia, Canada

*Corresponding authors: E-mails: alastair.simpson@dal.ca; andrew.roger@dal.ca.

Accepted: January 18, 2018

Data deposition: All new transcriptomic data have been deposited at the National Center for Biotechnology Information under BioProjects PRJNA401035, as detailed in supplementary table S1, Supplementary Material online. All single gene alignments, masked and unmasked, and phylogenomic matrices are available in supplementary file, Supplementary Material online [Brown_et al.2017.CRuMs.tgz](#).

Abstract

Recent phylogenetic analyses position certain “orphan” protist lineages deep in the tree of eukaryotic life, but their exact placements are poorly resolved. We conducted phylogenomic analyses that incorporate deeply sequenced transcriptomes from representatives of colodictyonids (diphylleids), rigifilids, *Mantamonas*, and ancyromonads (planomonads). Analyses of 351 genes, using site-heterogeneous mixture models, strongly support a novel super-group-level clade that includes colodictyonids, rigifilids, and *Mantamonas*, which we name “CRuMs”. Further, they robustly place CRuMs as the closest branch to Amorphea (including animals and fungi). Ancyromonads are strongly inferred to be more distantly related to Amorphea than are CRuMs. They emerge either as sister to malawimonads, or as a separate deeper branch. CRuMs and ancyromonads represent two distinct major groups that branch deeply on the lineage that includes animals, near the most commonly inferred root of the eukaryote tree. This makes both groups crucial in examinations of the deepest-level history of extant eukaryotes.

Key words: eukaryote tree of life, concatenated phylogenetic analysis, protist, site-heterogeneous models.

Introduction

Our understanding of the eukaryote tree of life has been revolutionized by genomic and transcriptomic investigations of diverse protists, which constitute the overwhelming majority of eukaryotic diversity (Burki 2014; Simpson and Eglit 2016). Phylogenetic analyses of super-matrices

of proteins typically show a eukaryote tree consisting of five-to-eight “super-groups” that fall within three even-higher-order assemblages: 1) Amorphea (Amoebozoa plus Obazoa, the latter including animals and fungi), 2) Diaphoretickes (primarily Sar, Archaeplastida, Cryptista, and Haptophyta), and 3) Excavata (Discoba

and Metamonada) (Adl et al. 2012). Recent analyses (Derelle et al. 2015) place the root of the eukaryote tree somewhere between Amorphea and the other two listed lineages; Derelle *et al.* (2015) termed this the “Opimoda-Diphoda” root. There is considerable debate over the position of the root, however (Cavalier-Smith 2010; Katz et al. 2012; He et al. 2014).

Nonetheless, there remain several “orphan” protist lineages that cannot be assigned to any super-group by cellular anatomy or ribosomal RNA phylogenies (Brugerolle et al. 2002; Glücksman et al. 2011; Heiss et al. 2011; Cavalier-Smith 2013; Pawlowski 2013; Yabuki, Ekrem, et al. 2013; Yabuki, Ishida, et al. 2013; Katz and Grant 2015). Recent phylogenomic analyses including *Colloctycon*, *Mantamonas*, and ancyromonads indicate that these particular “orphans” branch near the base of Amorphea (Zhao et al. 2012; Cavalier-Smith et al. 2014), the same general position as the purported Opimoda-Diphoda root. This implies, 1) that these lineages are of special evolutionary importance, but also, 2) that uncertainty over their phylogenetic positions will profoundly impact our understanding of deep eukaryote history. Unfortunately their phylogenetic positions indeed remain unclear, with different phylogenomic analyses supporting incompatible topologies, and often showing low statistical support (Cavalier-Smith et al. 2014). This is likely due in part to the modest numbers of sampled genes for some/most species and generally poor taxon sampling (Cavalier-Smith et al. 2014; Torruella et al. 2015). Therefore, we undertook phylogenomic analyses that incorporated deeply sequenced transcriptome data from representatives of two colloctyconids, a *Mantamonas*, three ancyromonads, and a single rigifilid.

Materials and Methods

Details of experimental methods for culturing, nucleic acid extraction, and Illumina sequencing are described in the supplementary text, [Supplementary Material](#) online.

Phylogenomic Data Set Construction

A reference data set of 351 aligned proteins described in (Kang et al. 2017) was used as the starting point for the current analysis, from which 61 or 64 taxa representing diverse eukaryotes were selected (see [supplementary table S2, Supplementary Material](#) online). Extensive efforts were made to exclude contamination and paralogs, as described in the supplementary text, [Supplementary Material](#) online. Poorly aligned sites were excluded using BMGE (Criscuolo and Gribaldo 2010), resulting in an alignment of 97,002 amino acid (AA) sites with <25% missing data for both 61- and 64-taxon data sets ([supplementary table S2, Supplementary Material](#) online).

Phylogenomic Tree Inference

Maximum likelihood (ML) trees were inferred using IQ-TREE v. 1.5.5 (Nguyen et al. 2015). The best-fitting available model based on the Akaike Information Criterion (AIC) was the LG + C60 + F+ Γ mixture model with class weights optimized from the data set and four discrete gamma (Γ) categories. ML trees were estimated under this model for both 61- and 64-taxon data sets. We then used this model and best ML tree under the LG + C60 + F+ Γ model to estimate the “posterior mean site frequencies” (PMSF) model (Wang et al. 2017) for both 61 (fig. 1) and 64 ([supplementary fig. S1, Supplementary Material](#) online) taxon data sets. This LG + C60 + F+ Γ -PMSF model was used to re-estimate ML trees, and for a bootstrap analysis of the 61-taxon data set, with 100 pseudoreplicates (fig. 1). AU topology tests under the LG + C60 + F+ Γ were conducted with IQ-TREE to evaluate whether trees recovered by the Bayesian analyses or alternative placements (see [supplementary table S1, Supplementary Material](#) online, for hypotheses tested) of the orphan taxa could be rejected statistically.

Bayesian inferences were performed using PHYLOBAYES-MPI v1.6j (Rodrigue and Lartillot 2014), under the CAT-GTR+ Γ model, with four discrete Γ categories. For the 61-taxon analysis, 6 independent Markov chain Monte Carlo chains were run for ~4,000 generations, sampling every second generation. Two sets of two chains converged (at 800 and 2,000 generations, which were, respectively, used as the burnin), with the largest discrepancy in posterior probabilities (PPs) (maxdiff) < 0.05. The topologies of the converged chains are presented in supplementary figures S3 and S4, [Supplementary Material](#) online, and are mapped upon figure 1. For the 64-taxon analysis, four chains were run for ~3,000 generations. Two chains converged at ~200 generations, which was used as the burnin, (maxdiff = 0) and the posterior probabilities are mapped upon the ML tree in [supplementary figure S1, Supplementary Material](#) online.

Fast-Site Removal and Gene Subsampling Analyses

For fast site removal, rates of evolution at each site of the 61-taxon data set were estimated with DIST_EST (Susko et al. 2003) under the LG model using discrete gamma probability estimation. A custom PYTHON script was then used to remove fastest evolving sites in 4,000-site steps. Random subsampling of 20%, 40%, 60%, or 80% of the genes in the 61-taxon data set was conducted using a custom PYTHON script, with the number of replicates as given in figure 2B. In both cases each step or subsample was analyzed using 1,000 UFBOOT replicates in IQ-TREE under the LG + C60 + F+ Γ -PMSF model.

Results

Using a custom phylogenomic pipeline plus manual curation, we generated a data set of 351 orthologs. The data set was

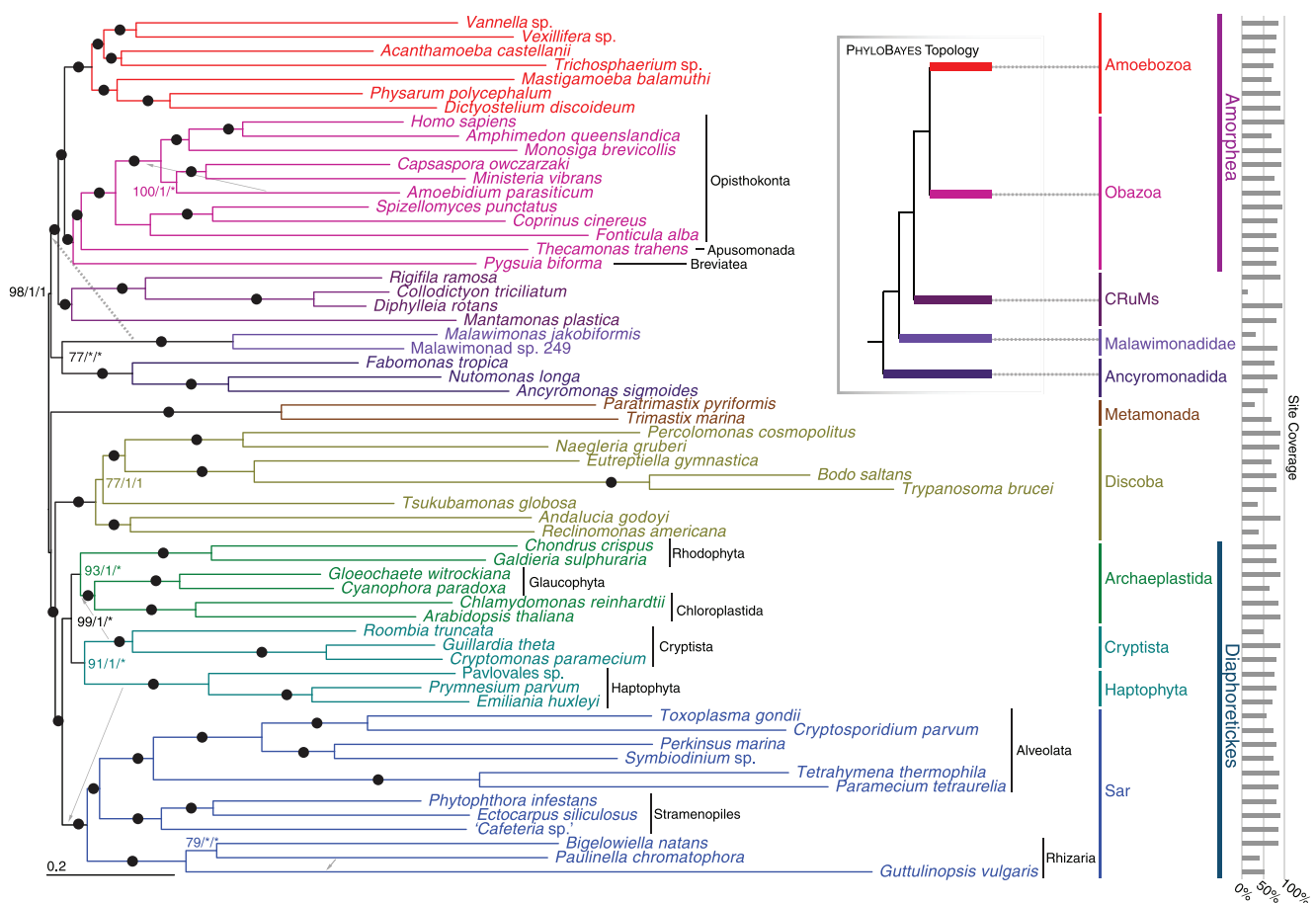


Fig. 1.—Phylogenetic tree for 61 eukaryotes, inferred from 351 proteins using Maximum Likelihood (LG + C60 + F+Γ-PMSF model). The numbers on branches show (in order) support values from 100 real bootstrap replicates (LG + C60 + F+Γ-PMSF model) and posterior probabilities from both sets of converged chains in PHYLOBAYES-MPI under CAT-GTR+Γ model (i.e., MLBS/PP/PP). Filled circles represent maximum support with all methods; asterisks indicate a clade not recovered in the PHYLOBAYES analysis. The dashed arrow indicates the placement of malawimonads inferred with PHYLOBAYES-MPI (see also inset summary tree), and gray arrows indicate the placements of other lineages in the PHYLOBAYES-MPI analyses.

filtered of paralogs and potential cross-contamination by visualizing each protein’s phylogeny individually, then removing sequences whose positions conflicted with a conservative consensus phylogeny (as in Tice et al. 2016; Kang et al. 2017) (supplementary methods, Supplementary Material online). We selected data-rich species to represent the phylogenetic diversity of eukaryotes. Our primary data set retained 61 taxa, with metamonads represented by two short-branching taxa (*Trimastix* and *Paratrimastix*). We also analyzed a 64-taxon data set containing three additional longer branching metamonads. Maximum likelihood (ML) and Bayesian analyses were conducted using site-heterogeneous models; LG + C60 + F+Γ and the associated PMSF model (LG + C60 + F+Γ-PMSF) as implemented in IQ-TREE (Wang et al. 2017) and CAT-GTR+Γ in PHYLOBAYES-MPI, respectively. Such site-heterogeneous models are important for deep-level phylogenetic inference with numerous substitutions along branches (Lartillot et al. 2007; Le et al. 2008; Wang et al. 2008, 2017; Pisani et al. 2015).

Our analyses of both 61- and 64-taxon data sets robustly recover well-accepted major groups including Sar, Discoba, Metamonada, Obazoa, and Amoebozoa (fig. 1 and supplementary fig. S1, Supplementary Material online). Cryptista (e.g., cryptomonads and close relatives) branches with Haptophyta (fig. 1) in the LG + C60 + F+Γ-PSMF analyses as well as in one set of two converged PHYLOBAYES-MPI chains under the CAT-GTR model (supplementary fig. S2, Supplementary Material online). However another pair of converged chains places Haptophyta as sister to Sar while Cryptista nests within Archaeplastida (supplementary fig. S3, Supplementary Material online), which is largely consistent with some other recent phylogenomic studies (Burki et al. 2016). Excavata was never monophyletic, with Discoba forming a clan with Diaphoretickes taxa (Sar, Haptophyta, Archaeplastida + Cryptista) and Metamonada grouping with Amorphea plus the four orphan lineages targeted in this study (see below).

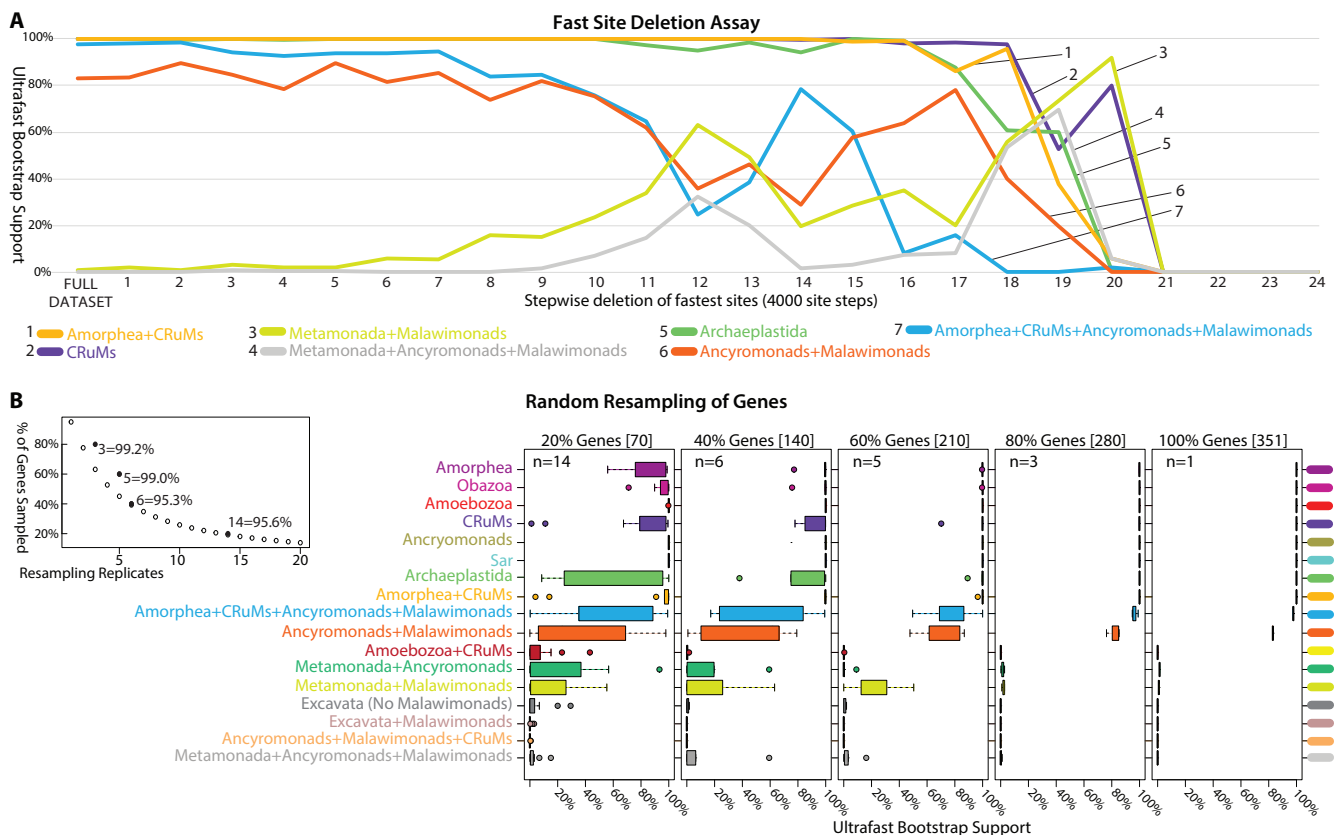


FIG. 2.—Effects of fast evolving sites and random subsampling of genes on our phylogenomic analyses. (A) Sites were sorted based on their rates of evolution estimated under the LG + F+Γ model and removed from the data set from highest to lowest rate. Each step has 4,000 of the fastest evolving sites removed progressively. The bootstrap values (UFBOOT; LG + C60 + F+Γ-PSMF model) for each bipartition of interest are plotted. (B and C) Effects of random subsampling of genes within the 351-gene data set. The following bipartitions were examined but received nearly 100% support across the fast site deletion series (data not shown); Amorphea, Obazoa, Amoebozoa, Ancyromonads, and Sar. The following bipartitions were examined but received nearly 0% support across the fast site deletion series (data not shown); Amoebozoa + CRuMs, Metamonada + Ancyromonads, Excavata (No Malawimonads), Excavata + Malawimonads, and Ancyromonads + Malawimonads + CRuMs. (B) Effects of random subsampling of genes on the bipartitions of interest. Inset panel is the calculation of the number of replicates (n) necessary for a 95% probability of sampling every gene when subsampling 20%, 40%, 60%, and 80% of genes using the formula: $0.95 = 1 - (1 - x/100)^n$, where x is the percentage of genes subsampled. UFBOOT support values for all nodes of interest with the variability of support values illustrated by box-and-whisker plots.

Malawimonads, which are morphologically similar to certain metamonads and discobids (Simpson 2003), also branch among the “orphans” (see below).

Phylogenies of both data sets place all four orphan taxa near the base of Amorphea (fig. 1 and supplementary fig. S1, Supplementary Material online). The uncertain position of the eukaryotic root (discussed earlier) therefore makes it unclear which bipartitions are truly clades, and which could be interrupted by the root. To allow efficient communication, we discuss the phylogenies as if the orphan taxa all lie on the Amorphea side of the root. We will also consider Amorphea as previously circumscribed (Adl et al. 2012): the least-inclusive clade or clan containing Amoebozoa and Opisthokonta.

Three of the orphan lineages are specifically related in our trees (fig. 1 and supplementary fig. S1, Supplementary Material online). In both 61- and 64-taxon analyses, *Rigifila ramosa* (representing Rigifilida) forms a maximally supported

clade with the collodictyonids *Collodictyon triciliatum* and *Diphylleia rotans*. *Mantamonas plastica* then branches as their closest relative, with maximal support. This Collodictyonid + Rigifilida + *Mantamonas* clade (“CRuMs”) forms the sister group to Amorphea, again with maximal support.

ML analyses and the converged PHYLOBAYES chains grouped ancyromonads, malawimonads, and CRuMs with Amorphea, with strong bootstrap support and Bayesian posterior probability (fig. 1, 61 taxa; PMSF BS = 98%, PP = 1). Ancyromonads and malawimonads formed a clade in the ML analyses, but with equivocal support (fig. 1, 61 taxa; BS = 77%). Both sets of converged chains of the Bayesian analyses instead grouped malawimonads with CRuMs + Amorphea to the exclusion of ancyromonads (supplementary figs. S2 and S3, Supplementary Material online, PP = 1 for both); however some unconverged chains support

an ancyromonad + malawimonad clade (data not shown). Lack of convergence among multiple chains using the CAT-GTR+ Γ model is unfortunately common for large data sets, and often cannot be resolved by increasing the number of generations of Markov chain Monte Carlo within a reasonable time frame (Pisani et al. 2015; Kang et al. 2017). Instead we treat the two topologies recovered in these analyses as candidate hypotheses requiring further investigation.

We conducted approximately unbiased (AU) topology tests on the 61-taxon data set under the LG + C60 + F+ Γ mixture model (supplementary table S1, Supplementary Material online). These tests rejected the Phylobayes trees, as well as all trees optimized by enforcing constraints representing plausible alternative relative placements of ancyromonads, malawimonads, and metamonads.

The fastest evolving sites are expected to be the most prone to saturation and systematic error arising from model misspecification in phylogenomic analyses (Philippe et al. 2011). We conducted a “fast-site removal” analysis with the 61-taxon data set and generated ultrafast bootstrap support (UFBOOT) values (Minh et al. 2013) for relevant groups as sites were progressively removed from fastest to slowest (fig. 2A). All groups of interest receive reasonably strong support until ~44,000–48,000 sites were removed, when support fell markedly for the ancyromonad + malawimonad clade and the Amorphea + CRuMs + ancyromonad + malawimonad clade. At this point, a notable proportion of the bootstrap trees show malawimonads and/or ancyromonads grouping with metamonads. This decline in support for the ancyromonad + malawimonad group reverses somewhat with further site removal, before support falls again as overall phylogenetic structure is lost when ~76,000 sites are removed (fig. 2A).

To evaluate heterogeneity in phylogenetic signals among genes (Inagaki et al. 2009), we also inferred phylogenies from subsamples of the 351 examined genes (61-taxon data set; fig. 2B and C). For each subsample 20–80% of the genes were randomly selected, without replacement, with replication as per figure 2B (giving a >95% probability that a particular gene would be sampled at each level), and UFBOOT support for major clades was inferred (fig. 2C). The “80% retained” replicates gave nearly identical results to the full data set, indicating that there was little stochastic error associated with gene sampling at this level. Support for the CRuMs clade is almost always high when 40%+ of genes are retained, whereas subsamples containing 60% of genes still showed differing support for an ancyromonad-malawimonad clade (as opposed to, e.g., malawimonads branching with metamonads).

We also investigated whether heterogeneity in amino acid composition among sequences in the data set had any impact on the branching order of the inferred phylogenies. Clustering on amino acid composition failed to recover any groupings that were inferred in our phylogenies (supplementary fig. S5,

Supplementary Material online). As an alternative approach, we conducted analyses on a data set with the amino acid sequences recoded into fewer states, an approach that has been shown to ameliorate compositional bias problems (Feuda et al. 2017). We recoded the concatenated amino acid sequences of our 61-taxon data set into four states based on the saturation bins of (Susko and Roger 2007). ML analyses of the recoded data set using the general-time-reversible (GTR)+C60 + F+ Γ model (with 4 states) recovered a phylogeny (supplementary fig. S6, Supplementary Material online) largely congruent with the foregoing analyses (e.g., fig. 1). Together, these analyses strongly suggest that our phylogenetic results cannot be attributed to sequences of similar amino acid composition being artificially grouped together and that compositional heterogeneity had minimal impact on our analyses.

Discussion

Our 351 protein (97,002 AA site) super-matrix places several orphan lineages in two separate clades emerging between Amorphea and all other major eukaryote groups. All methods recover a strongly supported clade comprising the free-swimming collodictyonid flagellates, the idiosyncratic filose protist *Rigifila* (Rigifilida), and the gliding flagellate *Mantamonas*. This clade is resilient to exclusion both of fast-evolving sites and of randomly selected genes. It is also consistently placed as the immediate sister taxon to Amorphea. This represents the first robust estimate of the positions of these three taxonomically poor but phylogenetically deep clades. Previous phylogenomic analyses placed collodictyonids in various positions, such as sister to either malawimonads or Amoebozoa, but often with low statistical support (Zhao et al. 2012; Cavalier-Smith et al. 2014). Placements of *Mantamonas* have varied dramatically. A recent phylogenomic study recovered a weak *Mantamonas* + collodictyonid clade in some analyses, but other analyses in the same study instead recovered a weak *Mantamonas* + ancyromonad relationship (Cavalier-Smith et al. 2014), and SSU + LSU rRNA gene phylogenies strongly grouped *Mantamonas* with apusomonads (Glücksman et al. 2011; Yabuki, Ishida, et al. 2013). Our study decisively supports the first of these possibilities. This is the first phylogenomic analysis incorporating Rigifilida: Previous SSU + LSU rRNA gene analyses recovered a negligibly supported collodictyonid + rigifilid clade, but not a relationship with *Mantamonas* (Yabuki, Ishida, et al. 2013).

Overall, the hypotheses that 1) collodictyonids, rigifilids, and *Mantamonas* form a major eukaryote clade, and 2) this clade is sister to Amorphea, are novel, plausible, and evolutionarily important. No name exists for this putative super-group, and it is obviously premature to propose a formal taxon. We suggest the place-holding moniker “CRuMs” (Collodictyonidae, Rigifilida, *Mantamonas*), which is euphonic and evokes the species-poor nature of these taxa.

Whether ancyromonads branch outside Amorphea or within it has been disputed (Paps et al. 2013; Cavalier-Smith et al. 2014). Our study strongly places ancyromonads outside Amorphea, more distantly related to it than are the CRuMs. Ancyromonads instead fall “among” the excavate lineages (Discoba, Metamonada, and Malawimonadidae). Resolving the relationships among “excavates” is extremely challenging (Hampl et al. 2009; Derelle et al. 2015), and this likely contributed to our difficulty in resolving the exact position of ancyromonads vis-à-vis malawimonads. A close relationship between ancyromonads and some/all excavates would be broadly consonant with the marked cytoskeletal similarity between *Ancyromonas* and “typical excavates” (Heiss et al. 2011). Certainly, our study flags ancyromonads as highly relevant to resolving relationships among excavates.

Both candidate positions for ancyromonads place them at the center of a crucial open question: locating the root of the eukaryote tree. As discussed earlier, the latest analyses (Derelle et al. 2015) locate the root between Discoba + Diaphoretickes (“Diphoda”) and a clade including Amorphea, collodictyonids, and malawimonads (“Opimoda”). Our phylogenies show the ancyromonad lineage emerging close to this split. One of the two positions we recovered would actually place ancyromonads either as the deepest branch within “Diphoda,” or the deepest branch within “Opimoda,” or even as sister to all other extant eukaryotes. This demonstrates the profound importance of including ancyromonads in future rooted phylogenies of eukaryotes, using data sets optimized for this purpose.

Supplementary Material

Supplementary data are available at *Genome Biology and Evolution* online.

Acknowledgments

The authors thank Tom Cavalier-Smith and Ed Glücksman (Oxford University) for supplying cultures strains B-70 (*Ancyromonas sigmoides*), NYK3C (*Fabomonas tropica*), and Bass1 (*Mantamonas plastica*). The part of this work conducted at Dalhousie University was supported by NSERC Discovery grants awarded to A.G.B.S. (298366-2014) and A.J.R. (2016-06792), respectively. A.J.R. also acknowledges the Canada Research Chairs program for support. This project was supported in part by the National Science Foundation (NSF) Division of Environmental Biology (DEB) grant 1456054 (<http://www.nsf.gov>), awarded to M.W.B. Mississippi State University’s High Performance Computing Collaboratory provided some computational resources. The part of this work conducted at the University of Tsukuba was supported by grants from the Japan Society for the Promotion of Science (JSPS; 15H05606 and 15K14591 awarded to R.K., 23117006 and 16H04826 awarded to Y.I.,

15H04411 awarded to K.I., and 15H05231 to T.H.) and by the “Tree of Life” research project (University of Tsukuba).

Literature Cited

- Adl SM, et al. 2012. The revised classification of eukaryotes. *J Eukaryot Microbiol.* 59(5):429–493.
- Brugerolle G, Bricheux G, Philippe H, Coffea G. 2002. *Collodictyon triciliatum* and *Diphylleia rotans* (= *Aulacomonas submarina*) form a new family of flagellates (Collodictyonidae) with tubular mitochondrial cristae that is phylogenetically distant from other flagellate groups. *Protist* 153(1):59–70.
- Burki F. 2014. The eukaryotic tree of life from a global phylogenomic perspective. *Cold Spring Harb Perspect Biol.* 6(5):a016147.
- Burki F, et al. 2016. Untangling the early diversification of eukaryotes: a phylogenomic study of the evolutionary origins of Centrohelida, Haptophyta and Cryptista. *Proc Biol Sci.* 283:20152802.
- Cavalier-Smith T. 2010. Kingdoms Protozoa and Chromista and the eozoan root of the eukaryotic tree. *Biol Lett.* 6(3):342–345.
- Cavalier-Smith T. 2013. Early evolution of eukaryote feeding modes, cell structural diversity, and classification of the protozoan phyla Loukozoa, Sulcozoa, and Choanozoa. *Eur J Protistol.* 49(2):115–178.
- Cavalier-Smith T, et al. 2014. Multigene eukaryote phylogeny reveals the likely protozoan ancestors of opisthokonts (animals, fungi, choanozoans) and Amoebozoa. *Mol Phylogenet Evol.* 81:71–85.
- Crisuolo A, Gribaldo S. 2010. BMGE (Block Mapping and Gathering with Entropy): a new software for selection of phylogenetic informative regions from multiple sequence alignments. *BMC Evol Biol.* 10:210.
- Derelle R, et al. 2015. Bacterial proteins pinpoint a single eukaryotic root. *Proc Natl Acad Sci U S A.* 112(7):E693–E699.
- Feuda R, et al. 2017. Improved modeling of compositional heterogeneity supports sponges as sister to all other animals. *Curr Biol.* 27(24):3864–3870.
- Glücksman E, et al. 2011. The novel marine gliding zooflagellate genus *Mantamonas* (Mantamonadida ord. n.: Apusozoa). *Protist* 162(2):207–221.
- Hampl V, et al. 2009. Phylogenomic analyses support the monophyly of Excavata and resolve relationships among eukaryotic “supergroups.” *Proc Natl Acad Sci U S A.* 106(10):3859–3864.
- He D, et al. 2014. An alternative root for the eukaryote tree of life. *Curr Biol.* 24(4):465–470.
- Heiss AA, Walker G, Simpson AGB. 2011. The ultrastructure of *Ancyromonas*, a eukaryote without supergroup affinities. *Protist* 162(3):373–393.
- Inagaki Y, Nakajima Y, Sato M, Sakaguchi M, Hashimoto T. 2009. Gene sampling can bias multi-gene phylogenetic inferences: the relationship between red algae and green plants as a case study. *Mol Biol Evol.* 26(5):1171–1178.
- Kang S, et al. 2017. Between a pod and a hard test: the deep evolution of amoebae. *Mol Biol Evol.* 34:2258–2270.
- Katz LA, Grant JR, Parfrey LW, Burleigh JG. 2012. Turning the crown upside down: gene tree parsimony roots the eukaryotic tree of life. *Syst Biol.* 61(4):653–660.
- Katz LA, Grant JR. 2015. Taxon-rich phylogenomic analyses resolve the eukaryotic tree of life and reveal the power of subsampling by sites. *Syst Biol.* 64(3):406–415.
- Lartillot N, Brinkmann H, Philippe H. 2007. Suppression of long-branch attraction artefacts in the animal phylogeny using a site-heterogeneous model. *BMC Evol Biol.* 7(Suppl 1):S4.
- Le SQ, Lartillot N, Gascuel O. 2008. Phylogenetic mixture models for proteins. *Philos Trans R Soc Lond B Biol Sci.* 363(1512):3965–3976.
- Minh BQ, Nguyen MAT, von Haeseler A. 2013. Ultrafast approximation for phylogenetic bootstrap. *Mol Biol Evol.* 30(5):1188–1195.

- Nguyen L-T, Schmidt HA, von Haeseler A, Minh BQ. 2015. IQ-TREE: a fast and effective stochastic algorithm for estimating maximum-likelihood phylogenies. *Mol Biol Evol.* 32(1):268–274.
- Paps J, Medina-Chacón LA, Marshall W, Suga H, Ruiz-Trillo I. 2013. Molecular phylogeny of unikonts: new insights into the position of apusomonads and ancyromonads and the internal relationships of opisthokonts. *Protist* 164(1):2–12.
- Pawlowski J. 2013. The new micro-kingdoms of eukaryotes. *BMC Biol.* 11:40.
- Philippe H, et al. 2011. Resolving difficult phylogenetic questions: why more sequences are not enough. *PLoS Biol.* 9(3):e1000602.
- Pisani D, et al. 2015. Genomic data do not support comb jellies as the sister group to all other animals. *Proc Natl Acad Sci U S A.* 112(50):15402–15407.
- Rodrigue N, Lartillot N. 2014. Site-heterogeneous mutation-selection models within the PhyloBayes-MPI package. *Bioinformatics* 30(7):1020–1021.
- Simpson AGB. 2003. Cytoskeletal organization, phylogenetic affinities and systematics in the contentious taxon Excavata (Eukaryota). *Int J Syst Evol Microbiol.* 53(6):1759–1777.
- Simpson AGB, Eglit Y. 2016. Protist diversification. In: Kliman RM, editor. *Encyclopedia of evolutionary biology*. Vol. 3. Amsterdam: Elsevier. p. 344–360.
- Susko E, Field C, Blouin C, Roger AJ. 2003. Estimation of rates-across-sites distributions in phylogenetic substitution models. *Syst Biol.* 52(5):594–603.
- Susko E, Roger AJ. 2007. On reduced amino acid alphabets for phylogenetic inference. *Mol. Biol. Evol.* 24(9):2139–2150.
- Tice AK, et al. 2016. Expansion of the molecular and morphological diversity of Acanthamoebidae (Centramoebida, Amoebozoa) and identification of a novel life cycle type within the group. *Biol Direct.* 11:69.
- Torruella G, et al. 2015. Phylogenomics reveals convergent evolution of lifestyles in close relatives of animals and fungi. *Curr Biol.* 25(18):2404–2410.
- Wang H, Minh B, Susko E, Roger AJ. 2017. Modeling site heterogeneity with posterior mean site frequency profiles accelerates accurate phylogenomic estimation. *Syst Biol.* doi: 10.1093/sysbio/syx068.
- Wang H-C, Li K, Susko E, Roger AJ. 2008. A class frequency mixture model that adjusts for site-specific amino acid frequencies and improves inference of protein phylogeny. *BMC Evol Biol.* 8:331.
- Yabuki A, Eikrem W, Takishita K, Patterson DJ. 2013. Fine structure of *Telonema subtilis* Griessmann, 1913: a flagellate with a unique cytoskeletal structure among eukaryotes. *Protist* 164(4):556–569.
- Yabuki A, Ishida K-I, Cavalier-Smith T. 2013. *Rigifila ramosa* n. gen., n. sp., a filose apusozoan with a distinctive pellicle, is related to *Micronuclearia*. *Protist* 164:75–88.
- Zhao S, et al. 2012. *Collodictyon*—an ancient lineage in the tree of eukaryotes. *Mol Biol Evol.* 29(6):1557–1568.

Associate editor: Laura Katz